

**Fracture Toughness Testing Results of
Borated Stainless Steels**



Structural Integrity Associates, Inc.

www.structint.com

Report No.: SIR-00-058
Revision No.: 0
Project No.: TNI-07
File No.: TNI-07-403
April 2000

**Fracture Toughness Testing Results of
Borated Stainless Steels**

Prepared for:

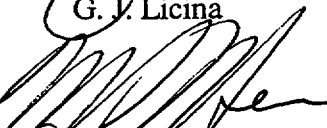
Transnuclear Incorporated
Hawthorne, NY

Prepared by:

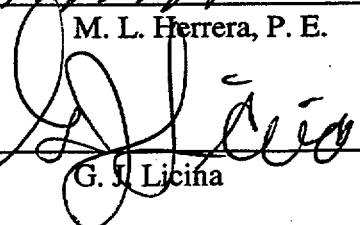
Structural Integrity Associates, Inc.
San Jose, California

Prepared by: 
G. J. Licina

Date: 4-24-00

Reviewed by: 
M. L. Herrera, P. E.

Date: 4/24/00

Approved by: 
G. J. Licina

Date: 4-24-00



REVISION CONTROL SHEET

Document Number: SIR-00-058

Title: Fracture Toughness Testing Results of Borated Stainless Steels

Client: Transnuclear, Inc.

SI Project Number: TNI-07

Section	Pages	Revision	Date	Comments
1.0	1-1 - 1-4	0	4/12/00	Initial Draft Issue
2.0	2-1			
3.0	3-1 - 3-2			
4.0	4-1 - 4-19			
5.0	5-1 - 5-4			
6.0	6-1 - 6-2			
7.0	7-1 - 7-2			



Table of Contents

<u>Section</u>	<u>Page</u>
1.0 BACKGROUND.....	1-1
2.0 OBJECTIVES	2-1
3.0 APPROACH	3-1
4.0 RESULTS.....	4-1
4.1 Tensile Properties.....	4-1
4.2 Impact Properties.....	4-2
4.3 Fracture Toughness Properties.....	4-2
4.4 Metallography and Fractography	4-3
5.0 DISCUSSION	5-1
6.0 CONCLUSIONS AND RECOMMENDATIONS.....	6-1
7.0 REFERENCES.....	7-1



List of Tables

<u>Table</u>	<u>Page</u>
Table 4-1 Tensile Properties of TN-BRP and TN-REG Materials	4-7
Table 4-2 Measured J-Integral Values from Westmoreland [4]	4-8
Table 4-3. Impact Test of Half-Size Charpy Specimens.....	4-9

List of Figures

<u>Figure</u>	<u>Page</u>
Figure 1-1. Fuel Baskets with Inserts for TN-REG and TN-BRP Casks (from [6]).....	1-4
Figure 3-1. REG Basket Plate E19 – L3 – N & S	3-2
Figure 4-1. Effect of Temperature on Yield Strength for Borated Stainless Steels	4-10
Figure 4-2. Effect of Temperature on Ultimate Strength of Borated Stainless Steels	4-11
Figure 4-3. Temperature Effects on Elongation of TN-REG and TN-BRP Materials.....	4-12
Figure 4-4. Room Temperature Fracture Toughness Values – Borated Stainless Steels	4-13
Figure 4-5. Fractography of TN-REG J_{Ic} Specimen	4-14
Figure 4-6. Fractography of TN-BRP J_{Ic} Specimen.....	4-15
Figure 4-7. Fractography of TN-REG J_{Ic} Specimen – High Power	4-16
Figure 4-8. Fractography of TN-BRP J_{Ic} Specimen – High Power.....	4-17
Figure 4-9. Metallography of TN-REG J_{Ic} Specimen	4-18
Figure 4-10. Metallography of TN-BRP J_{Ic} Specimen.....	4-19
Figure 5-1. Example of Correlations Between K_{Ic} and Charpy Impact Energy	5-4



EXECUTIVE SUMMARY

Tests of borated stainless steel plates from the fuel baskets for the Transnuclear TN-REG and TN-BRP shipping and storage casks have demonstrated that plates from both casks have reasonable ductility and fracture toughness.

Plates from the fuel baskets for the TN-REG and TN-BRP casks have shown that the ductility and toughness of borated stainless steels produced by Powder Metallurgy (PM) techniques are clearly superior to those from the ingot cast and wrought material.

The test program required to quantify the basket materials for one-time shipments included tensile tests, Charpy V-notch tests, and J-integral tests using small pre-notched and fatigue pre-cracked bent beams. The Charpy testing demonstrated that the material properties of these plates are consistent with the requirements of the applicable grades of ASTM A-887 borated stainless steel.

Experience with fracture testing of other grades of borated stainless steel has shown that the fracture toughness is too great to permit a valid direct measurement of K_{Ic} . Instead, elastic-plastic fracture properties (i.e., the J-integral) were determined vs. crack extension (Δa) as outlined in ASTM E-813 and E-1737 to define the limiting J value (J_{Ic}). From that J_{Ic} , and a K_{Ic} was determined by calculation.

Consistent with the literature, temperature appears to exert only a minor effect on tensile strength and ductility for the temperature range of interest (-20°F to +500°F). Temperature effects are less for the borated stainless steels than for standard grades such as Type 304L.

Charpy impact test results for half-size Charpy specimens from the TN-REG and TN-BRP materials were consistent with the requirements of ASTM A-887. For the highest boron content materials, the required Charpy impact energy is not very high (about 14 ft-lbs at -20°F).



Measurements of J_{Ic} at -20°F ranged from 116 in-lb/in² to 132 in-lb/in² for the TN-BRP material and 238 in-lb/in² to about 300 in-lb/in² for the TN-REG material. Corresponding K_{Ic} values are 62.4 ksi $\sqrt{\text{in}}$ to 66.4 ksi $\sqrt{\text{in}}$ for the TN-BRP material and 89.4 ksi $\sqrt{\text{in}}$ to 100.4 ksi $\sqrt{\text{in}}$ for the TN-REG material. The measured J_{Ic} values were in very good agreement with values for similar grades, where the associated K_{Ic} 's range from about 65 to about 125 ksi $\sqrt{\text{in}}$.

All of these measured values of toughness indicate that a reasonable level of toughness would be expected for both the ingot metallurgy material with 1.45% boron (TN-BRP basket) and for the PM material with 2.2% boron (TN-REG)

Optical metallographic examination of the TN-REG and TN-BRP basket materials also demonstrated boride sizes and distributions that were consistent with those reported in the literature, and confirmed that boride morphology, dimensions, and distributions were consistent within a product form.



1.0 BACKGROUND

Structural Integrity Associates report SIR-00-019 [1] describes the design of the Transnuclear TN-REG and TN-BRP transport and storage casks, describes NRC concerns with the borated stainless steel used for the cask internals, and provides recommendations for demonstrating that the borated stainless steel possesses adequate fracture toughness for use under potentially dynamic loads.

Safety Analysis Reports for the TN-REG and TN-BRP casks submitted to the NRC in 1985 for certification as Type B containers had been rejected. The analyses were rejected by the NRC at that time because:

1. Borated stainless steel had no established materials standard (e.g., ASTM)
2. No accepted codes or standards existed for acceptance of borated stainless steel as a structural material for loading conditions that include a 30 foot drop (per 10CFR71, a standard for shipping container containment)
3. Charpy impact data for borated stainless steel were significantly below the values generally associated with austenitic stainless steels. As such, the borated stainless steels were considered to possess inadequate toughness for use in an application such as these transport and storage casks.

The NRC's rejection noted that the following future work would be required to qualify the casks:

1. Borated stainless steel must be covered by an ASTM specification
2. Allowable stresses for borated stainless steel under normal and accident conditions must be defined in a consensus code standard
3. Fatigue and fracture must be addressed by the standard. Brittle fracture must be avoided by use of sufficiently ductile and tough material.
4. Analysis or testing must demonstrate that stresses are within specified limits for all loadings and orientations.

As an interim measure, the basket designs were altered so that the payload would always be kept subcritical without taking any credit for the borated stainless steel as a structural material. This



was done by shipping the cask half full of fuel with inserts in the empty slots in a checkerboard pattern and along the periphery (Figure 1-1). Those structural inserts are full length, diagonally braced box beams (SA-240, XM-19), constructed from 5 individual segments joined by pinned adapters/flexible joints.

Subsequent analyses of the overall safety of the shipping and storage process suggested that the overall safety would be enhanced by qualifying the cask inserts for a single shipment and using the casks only once rather than using the partially loaded casks with modified internals for multiple shipments.

Since the original application for cask certification, materials specification ASTM A-887-88 [2] was issued (August 26, 1988). It includes 8 types of borated stainless steel plates based on the amount of boron (from Type 304B with 0.2% to 0.3%) to Type 304B7 (1.75% to 2.25%). For each Type, there are two Grades (A and B), defined by tensile elongation. In practice, Type A is plate produced by powder metallurgy techniques; Type B is a wrought product produced by conventional ingot metallurgy.

Transnuclear, the United States Department of Energy, and Structural Integrity Associates presented a review of the cask designs, cask insert loadings, and a proposed test program to assuage the NRC's concerns regarding fracture toughness of the borated stainless steel, and to ultimately qualify the casks for single shipments. A key part of that presentation focused on the predicted fracture toughness of the borated stainless steel and methods to measure the actual mechanical properties of the plates removed from the TN-REG and TN-BRP baskets. Those properties determinations are reported in Reference 3 and are summarized and discussed in this report.

The qualification test program that was proposed to quantify and bound the actual fracture toughness of the basket materials included Charpy V-notch tests, tensile tests, and J-integral tests (e.g., small pre-notched and fatigue pre-cracked bent beams). The tensile testing was included to verify the effect of temperature on tensile properties and to provide critical strength parameters for determination of the J_{Ic} . Charpy impact testing was expected to demonstrate that the material



properties are consistent with the requirements of ASTM A-887; alloys for which the fracture toughness has been shown to be too great to permit a valid, direct measurement of K_{Ic} . Instead, single specimen J_{Ic} determinations would be made (i.e., J vs. Δa) as outlined in ASTM E-813 [4] and E-1737 [5] such that a limiting J value (J_{Ic}) can be determined.

From that measured J_{Ic} , a K_{Ic} value can be calculated for comparison to the linearly elastic stress intensity factor, the applied K determined from the stresses in the design analyses and postulated or measured flaws. An analytical demonstration that conservatively calculated applied K's are less than K_{Ic} for all loading conditions provides the assurance that brittle fracture will be avoided.

Finally, the proposed test program included metallography and fractography to demonstrate that typical material samples had been selected, and to characterize grain size, boride morphology and distribution, and the modes of fracture.



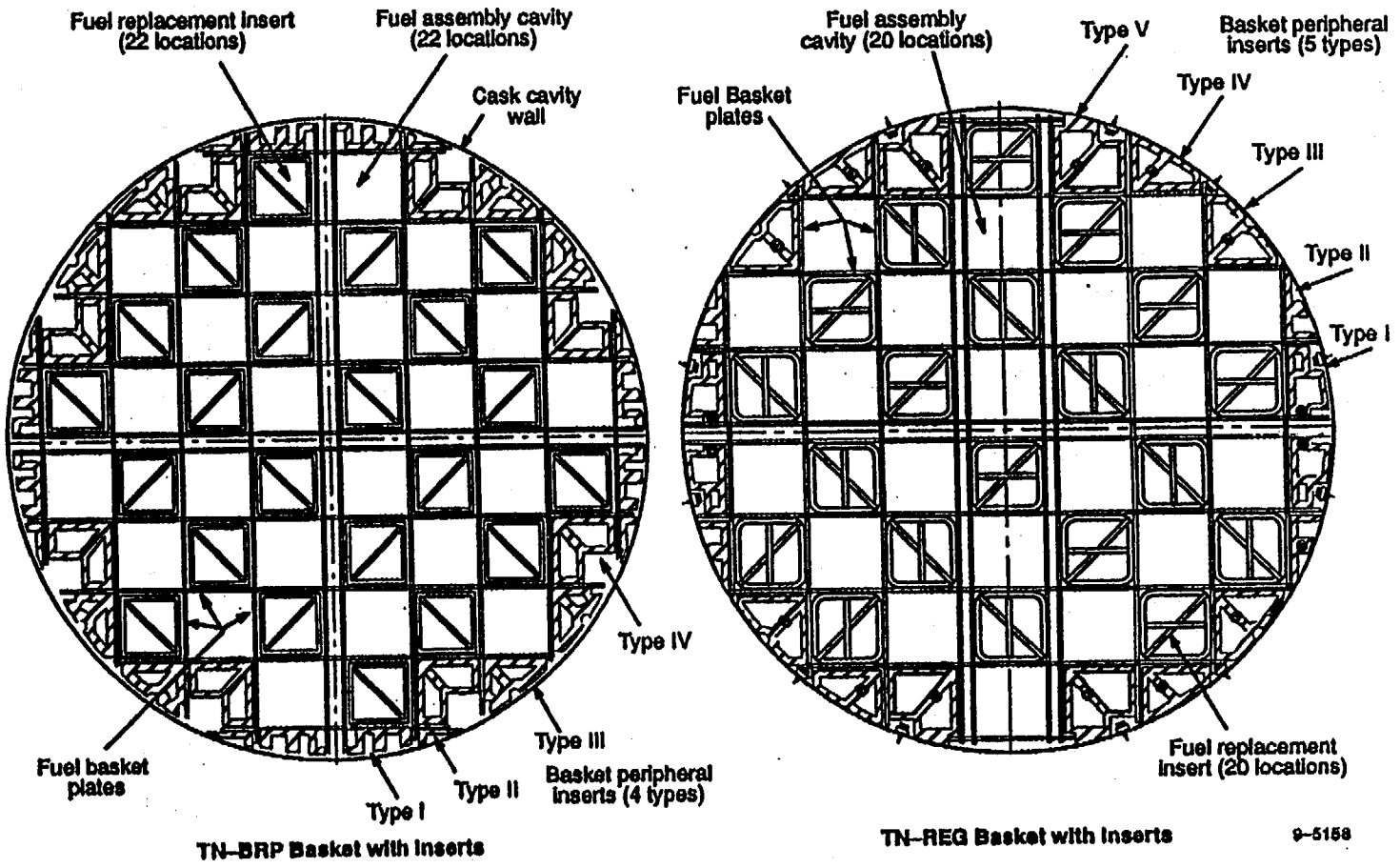


Figure 1-1. Fuel Baskets with Inserts for TN-REG and TN-BRP Casks (from [6])



2.0 OBJECTIVES

The objective of this work was to evaluate the results of mechanical properties measurements made by Westmoreland Mechanical Testing & Research [3] on specimens from actual basket plates from the TN-REG and TN-BRP casks. The primary focus was on the fracture toughness properties and microstructure of the materials.



3.0 APPROACH

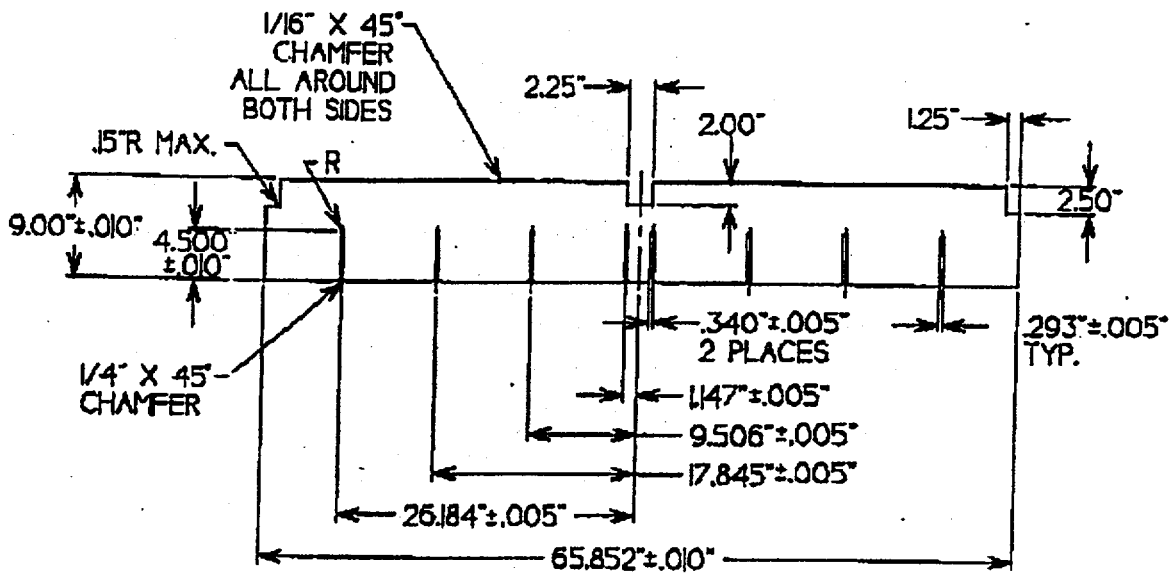
Following a detailed review of reports on the physical metallurgy and mechanical properties of borated stainless steels, summarized in Reference 1, a test program to address the data needs was formulated and presented to the NRC for their concurrence. Actual plates from the TN-REG and TN-BRP baskets were used as starting stock for all tests.

Plates 7J-2 (LN3, Can C1965) and 7J-1 (LN3, Can C1965) were removed from the E19 layer of the TN-REG basket (Figure 3-1). These plates were called REG Pieces 1 and 2 by Westmoreland. Plates 116/2-125 (L3) and 78/3-127 (L5) were removed from the E19 layer of the TN-BRP basket.¹ They were designated BRP Pieces 1 and 2 by Westmoreland.

The program included tensile and Charpy impact tests (of sub-size specimens), notched and pre-cracked bent beams for determinations of J_{Ic} , and fractographic and metallographic examinations. Tensile specimens were oriented in the transverse direction and tested at -20°F , room temperature, and elevated temperature (either 400°F or 500°F). Charpy specimens and notched and pre-cracked bent beams for J_{Ic} testing were machined from the plates to produce a T-L orientation (axis of specimen in the transverse direction; crack propagation along the longitudinal direction). Those orientations provide the most conservative results.

The objective of the program was to characterize the fracture toughness of the borated stainless steel and to include a reasonable description of the variability of those properties.

¹Per the CMTRs, plates 116/2 and 78/3 come from length groups LN3 and LN5. See Table 1-1 of [1].



REG BASKET PLATE E19 - L3 - N & S

PLATE THICKNESS - $.276^{+.010}_{-.015}$
 TOLERANCE (UNSPECIFIED) $XX = \pm .03$
 ANGLES ± 2

Figure 3-1. REG Basket Plate E19 - L3 - N & S

4.0 RESULTS

4.1 Tensile Properties

The primary objective of the tensile tests was to determine the temperature dependence of the tensile properties for the TN-BRP and TN-REG materials. Results are summarized in Table 4-1.

Results for the TN-BRP and TN-REG materials are plotted in Figures 4-1, 4-2, and 4-3. The temperature dependence of the tensile properties of other grades of borated stainless steels are shown for comparison. The tensile properties of the TN-REG material, shown as solid circles, are in very good agreement at all temperatures with those from both the 304B6A and 304B7A grades, the PM materials with the highest boron contents. The ultimate tensile strength and temperature dependence of the ultimate strength for the TN-BRP material (filled squares) are slightly less than those for a 304B4A material but greater than those for 304B3B (ingot metallurgy) material with a lower boron content. The yield strength of the TN-BRP material was very similar to that of the TN-REG material at all temperatures. The tensile elongations of the TN-BRP and TN-REG materials are similar to each other, despite the significant differences in boron contents for the two plates. Those elongation values are fairly consistent with those for the 304B7A material; better than what would have been predicted for the TN-BRP plates.

As noted in SIR-00-019 [1], the chromium and iron borides that form during primary processing persist to room temperature and affect ductility and toughness dramatically. The final particle size and shape are set by the as-cast boride size and by the amount of work put into the metal during processing. In material produced by conventional ingot metallurgy, the size of the M_2B precipitates will be larger and less uniform and can have some directionality. In the powder metallurgy product, borides are smaller and more spherical, typically from 1 to 6 μ m. One characteristic of boron in stainless steel is to produce very fine grain sizes, as grain boundaries are pinned by the presence of a fine dispersion of those particles.

As shown in Figures 4-1 through 4-3, the mechanical properties of the TN-REG and TN-BRP are very consistent with the mechanical properties described in the properties characterization work



performed by Sandia in support of the ASME Section III Code case on borated stainless steel (ASTM A-887) for all 16 grades of material (boron contents from 0.20% to 2.25%) [7]. Consistent with that work, the TN-REG and TN-BRP plates show that tensile strengths increase with boron content and ductilities decrease with increasing boron content.

4.2 Impact Properties

As would be expected for the high boron content material, the Charpy impact properties were low. The available sections did not permit the construction of full size Charpy specimens. Half size specimens were tested instead. Those half size specimens, tested at -20°F failed at absorbed impact energies of 4 ft-lbs for the TN-BRP material (1.43% boron; ingot metallurgy) and 7 ft-lbs for the TN-REG material (2.22% boron; powder metallurgy), Table 4-3. Although there is no direct correlation to estimate impact properties for a full size sample from a sub-size sample, for these materials, stainless steels that exhibit ductile tearing of the matrix between the hard boride particles and cleavage of the particles themselves, doubling the impact energy of a half-size specimen appears to be justified. Note that the Charpy impact properties are not quantitative and are not used as a design property.

4.3 Fracture Toughness Properties

Based on results from other mechanical properties tests on borated stainless steels indicating some ductility, direct determinations of K_{Ic} were considered impractical because the material was too tough to permit direct measurement of K_{Ic} on this section. The use of elastic-plastic fracture methods, specifically the J-integral, were used. Results from 0.250 inch thick notched and pre-cracked bent beams fabricated from TN-REG and TN-BRP plates are summarized in Table 4-2 and Figure 4-4.

As described in [3], the J_{Ic} tests were done in accordance with ASTM E-1737 on fatigue pre-cracked, notched bend bars about 0.250 inches thick. The specimens were side grooved to 10% of their thickness (0.025 inches for these specimens) after pre-cracking. As agreed with Gerry Boice, Westmoreland would attempt to determine valid J_{Ic} values using a single specimen



technique. They have been very successful with the single specimen method with a variety of materials in the past. At worst, if unsuccessful, the specimen tested would serve as one specimen of a multiple specimen test series. The J_{Ic} tests were done on an Instron test frame (Westmoreland machine #H53) at $-20^{\circ}\text{F} \pm 2^{\circ}\text{F}$ with specimens immersed in methanol and liquid nitrogen to maintain the desired temperature.

Six of the seven J_{Ic} tests that were run met all of the validity criteria of ASTM -1737. The only sample that failed to meet all of the validity criteria was the first test of the TN-BRP plate. Like the first TN-REG plate specimen and all of the subsequent tests, the first TN-BRP test produced well-behaved data. The test was considered invalid, but only because the number of points used to define the fit along the blunting line was less than the 8 required. All of the other validity criteria were met and the data looked well behaved. The J_Q (tentative J_{Ic} subject to validity determinations) was 124.6 in-lb/in^2 . The reason that less than 8 points were used was because the J vs. Δa curve "bent over", that is, it deviated from the blunting line, at a low load/ Δa . Subsequent runs on TN-BRP materials were performed using a slightly modified technique that unloaded the sample every 0.5 mil of crack extension vs. the 1 mil that is typically used for these tests.

As shown in Table 4-2, the variability in the J_{Ic} determined for each plate material was very small; a maximum of about 12% for the TN-REG material; about 8% the TN-BRP material.

Table 4-2 also includes determinations of K_{Ic} from values of J_{Ic} using the expression

$$J_{Ic} = \frac{K_{Ic}^2(1 - \nu^2)}{E}$$

Table 4-2 shows that for the TN-REG plate, a lower bound K_{Ic} (mean - two standard deviations) of 89 ksi $\sqrt{\text{in}}$ should be used. For the TN-BRP plate, the lower bound K_{Ic} would be 62.8 ksi $\sqrt{\text{in}}$.

4.4 Metallography and Fractography

Fractography is done as a routine part of the J_{Ic} analysis. Figures 4-5 through 4-8 show typical examples of the fracture surfaces. Three distinct zones are visible for each J_{Ic} specimen: the



fatigue pre-crack area, the crack extension produced during the J_{IC} test, and the rapid final fracture. The final fracture was obvious since it had not been heat tinted. The fatigue pre-crack and the crack extension area were both turned a light golden color by the 650°F heat tint.

The fractography of the REG sample clearly showed the fatigue pre-crack and tear zones (Figure 4-5). Examination in the SEM (Figure 4-7) revealed that the crack extension from the J test appeared to produce a completely ductile tearing of the austenite matrix and cleavage of the many apparently spherical boride particles. There was no evidence of any cracking or intergranular fracture in the crack extension zone. The heat tinting procedure used by Westmoreland (about 650°F for 20-30 minutes) gave the heat tinted area a light golden colored that contrasted with the final fracture, produced by cooling the specimen in liquid nitrogen (about -320°F) and breaking it open by hitting it with a hammer. Macroscopically and microscopically, the final fracture area did not look appreciably different from the area of stable crack extension from the J test other than the final fracture zone had no heat tint.

The fracture surfaces of the BRP sample were definitely different from those of the REG material (Figures 4-6 and 4-8). The boride particles in the BRP material were much larger and elongated. Those fractured particles appeared as dark streaks on the fracture surface at relatively low magnification (Figure 4-6). The austenite matrix of the BRP material still had an essentially 100% ductile nature to it, however, the scale of everything (borides and apparent austenite grains) was much more coarse than that of the REG material. The austenite matrix of the BRP material may have been somewhat elongated rather than equiaxed as the REG matrix material appeared to be.

Fractography of the crack extension zone of the J specimens of BRP material showed a much more coarse microstructure than for the REG. Low magnification SEM examination of that zone exhibited tears that corresponded to broken boride particles (Figure 4-8). Broken, elongated borides could also be seen in the fatigue pre-crack. Pre-cracking of the two materials (TN-BRP and TN-REG) was confirmed to have been done at the same loads, however, the Westmoreland technician had noticed that the TN-BRP material exhibited a more rapid crack growth than the



TN-REG, estimated to be about 20% faster. The faster crack growth rate was consistent with the differences in appearance of the pre-cracking zone for the two materials.

The Westmoreland report also included quantitative metallography of eight metallographic sections; 3 samples from two TN-REG plates and 5 samples from two TN-BRP plates. Figures 4-9 and 4-10 are typical examples. Westmoreland found that a KOH etchant worked best for them to define the boride particles with a minimum of interference from grain boundaries and other microstructural features.

The TN-REG material had a very uniform appearance (Figure 4-9). The boride particles were uniformly distributed and were very round. Although prior discussions had indicated that a "skin" of stainless steel with no borides might be present (i.e., from the can in which the powdered metals were hot pressed, then rolled), no evidence of any skin was seen. There was definitely no unbonded interface and only trace amounts of any surfaces with no borides. There was very minor evidence of small laps at the surface in one of the TN-REG specimens (#3). A search of all of the samples revealed only one area, less than about 0.3 mils thick, that was boride free and a layer maybe 3.9 mils thick that appeared to have a lower boride distribution.

The SEM and optical examinations suggested some evidence of very minor porosity in the TN-REG material.

Metallographically, the TN-BRP material was much different (Figure 4-10). The majority of the borides were elongated rather than round and the borides were much larger. Some of the very large boride particles had angular boundaries and not all of those boundaries were parallel or perpendicular to the rolling direction. The minor dimension of the elongated borides was probably larger than the diameter of the borides in the TN-REG material. The distribution of borides gave an almost banded appearance. That is, there were very distinct differences between fields of view. In some fields, there were lots of borides. In other fields, there were very few. In some fields borides were large or elongated; in others, borides were much finer. There may also have been small differences in boride volume fraction from one edge of the plate to the other. In summary, the borides in the TN-BRP material were far less homogeneous than in the TN-REG material.



The quantitative metallography performed by Westmoreland was based upon analyses of the maximum particle lengths and widths. For each sample, ten fields were examined at 500X. The number of particles was counted and the lengths and widths were analyzed statistically. The image analysis software assigns a length (maximum dimension) and width (minimum dimension) to each particle. The object sizes reported in the Westmoreland report are based upon the single maximum length and single maximum width determined for each of the ten fields counted for each metallographic sample. Those maximum values are not from the same particle and provide no real indication of the shape or aspect ratio of the particles.

Unfortunately, the values reported for the lengths and widths of the particles do not provide a clear indication of the differences between the TN-BRP and TN-REG materials. The appearance of the micrographs from the TN-REG material show that the vast majority of the boride particles are small and round and uniformly distributed. The ratio of the typical particle's length to its width appears to be essentially one. In addition, the typical size is fairly small and the size difference between the maximum and minimum particles appears to be minor. In contrast, most of the borides in the TN-BRP material are larger, are significantly longer than they are wide, perhaps a factor of 3 or 4, and the typical area or maximum dimensions of those particles is greater than that for the TN-REG material.

The metallographic work done by Westmoreland is considered extremely good. However, the reporting of the maximum length and width for the particles in each field does not provide a useful descriptor for the particles. Qualitative analysis of the borides is very possible from the published micrographs. The particle size numbers as reported should not be used for comparisons with other data in the literature (e.g., Robino and Cieslak [8]). Transnuclear may want to have Westmoreland re-analyze the micrographs and provide a better statistical descriptor of particle sizes. The use of the average lengths and widths or standard deviations for length and width in each field may be more useful.

Table 4-1
Tensile Properties of TN-BRP and TN-REG Materials

Alloy	Orient'n	%B	Temp, F	Yield Strength Ksi	Ultimate Strength ksi	Elong,%	RA, %
REG (1)-1	T	2.22	-20	62.9	133.3	17	12.3
REG (1)-2	T	2.22	-20	61.9	129.4	15	14.7
REG (1)-3	T	2.22	72	57.2	117	18	17.4
REG (1)-4	T	2.22	72	59.2	116.9	17	16.6
REG (1)-5	T	2.22	400	51.8	100.9	12	14.3
REG (1)-6	T	2.22	400	51.9	100.3	14	14.6
BRP (1)-7	T	1.43	-20	61	103	14	12.2
BRP (1)-8	T	1.43	-20	63	100.9	10	8.2
BRP (1)-9	T	1.43	72	58.9	93.9	12	10.5
BRP (1)-10	T	1.43	72	58.2	93.9	12	11
BRP (1)-11	T	1.43	500	52.1	79.5	8	6.9
BRP (1)-12	T	1.43	500	51.3	79.5	9	9.8

Table 4-2
Measured J-Integral Values from Westmoreland [4]

Alloy	%B	TL Orientation		Mean K_{IC}	S.D.	Mean-2(S.D.)
		J_{IC} in-lb/in ²	K_{IC} , ksi-sqrt(in)			
REG (1)-1	2.22	300.63	100.38			
REG (1)-2	2.22	238.54	89.41			
REG (1)-3	2.22	263.19	93.92			
				94.57	5.51	89.06
BRP (1)-7	1.43	124.6	64.62	Failed to meet all validity requirements		
BRP (1)-9	1.43	131.82	66.47			
BRP (1)-10	1.43	116.55	62.50			
BRP (1)-11	1.43	131.72	66.44			
				65.14	2.28	62.85

Values from [9] for Comparison

Alloy	%B	LT Orientation		TL Orientation	
		J_{IC} , in-lb/in ²	K_{IC} , ksi-sqrt(in)	J_{IC} , in-lb/in ²	K_{IC} , ksi-sqrt(in)
NeuroSorbPLUS	0.28	1945	255	1584	230
NeuroSorbPLUS	0.83	754	158	699	153
NeuroSorbPLUS	1.43	534	133	485	127
NeuroSorbPLUS	1.86	439	121	212	84
ASTM A887 Gr. B	1.07	344	107	277	96

All reported J_Q or J_{IC} values are assumed = J_{IC}

Table 4-3.
Impact Test of Half-Size Charpy Specimens

Sample	Orientation	%B	Impact Energy T, F	ft-lbs
BRP(1)-4	TL	1.43	-20	8
BRP(1)-5	TL	1.43	-20	8
BRP(1)-6	TL	1.43	-20	8
REG (1)-1	TL	2.22	-20	14
REG (1)-2	TL	2.22	-20	14
REG (1)-3	TL	2.22	-20	14

Effect of Temperature on Yield Strength

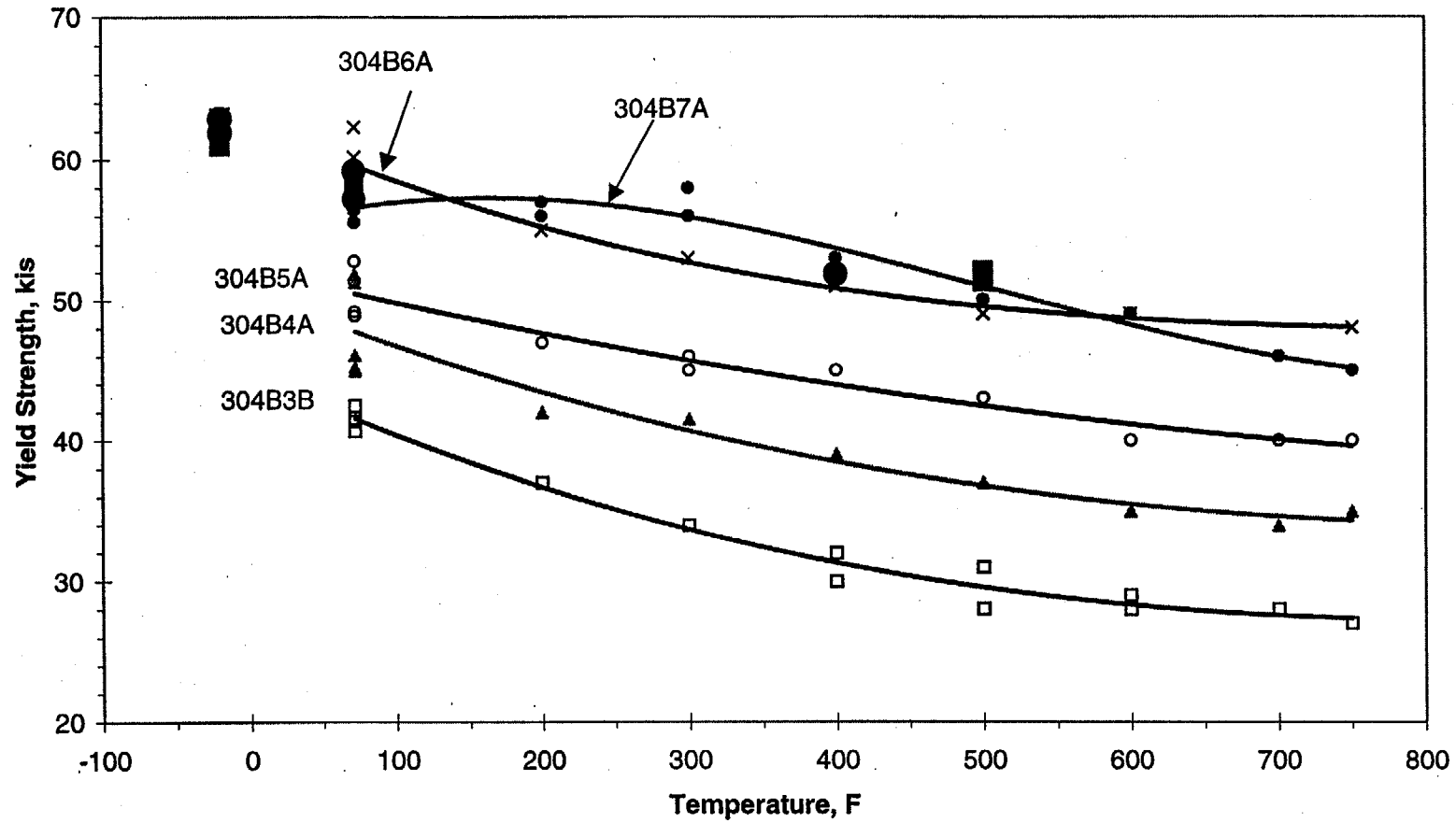


Figure 4-1. Effect of Temperature on Yield Strength for Borated Stainless Steels (from [2])



Effect of Temperature on Ultimate Strength

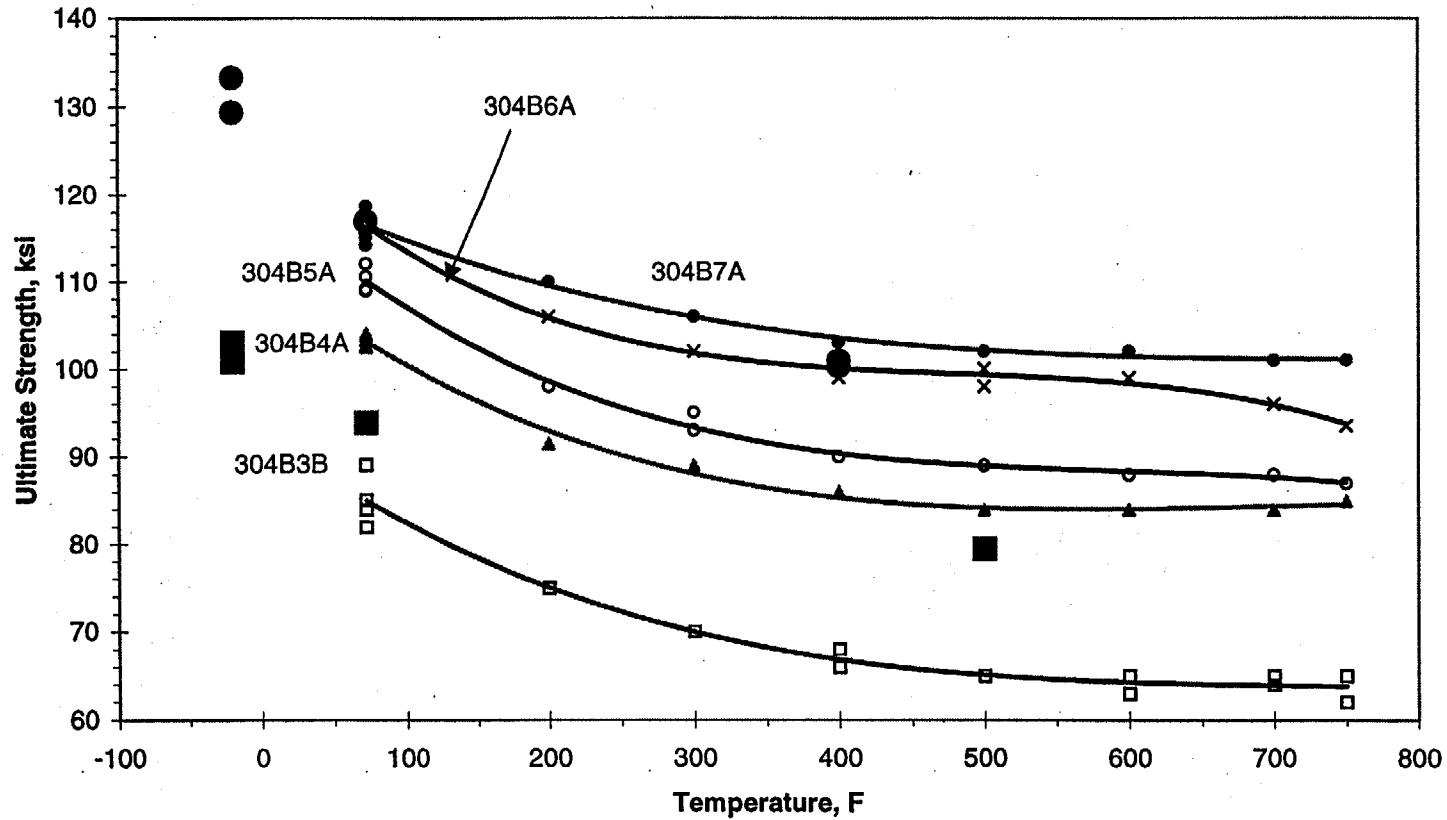


Figure 4-2. Effect of Temperature on Ultimate Strength of Borated Stainless Steels (from [2])

Effect of Temperature on Uniform Strain

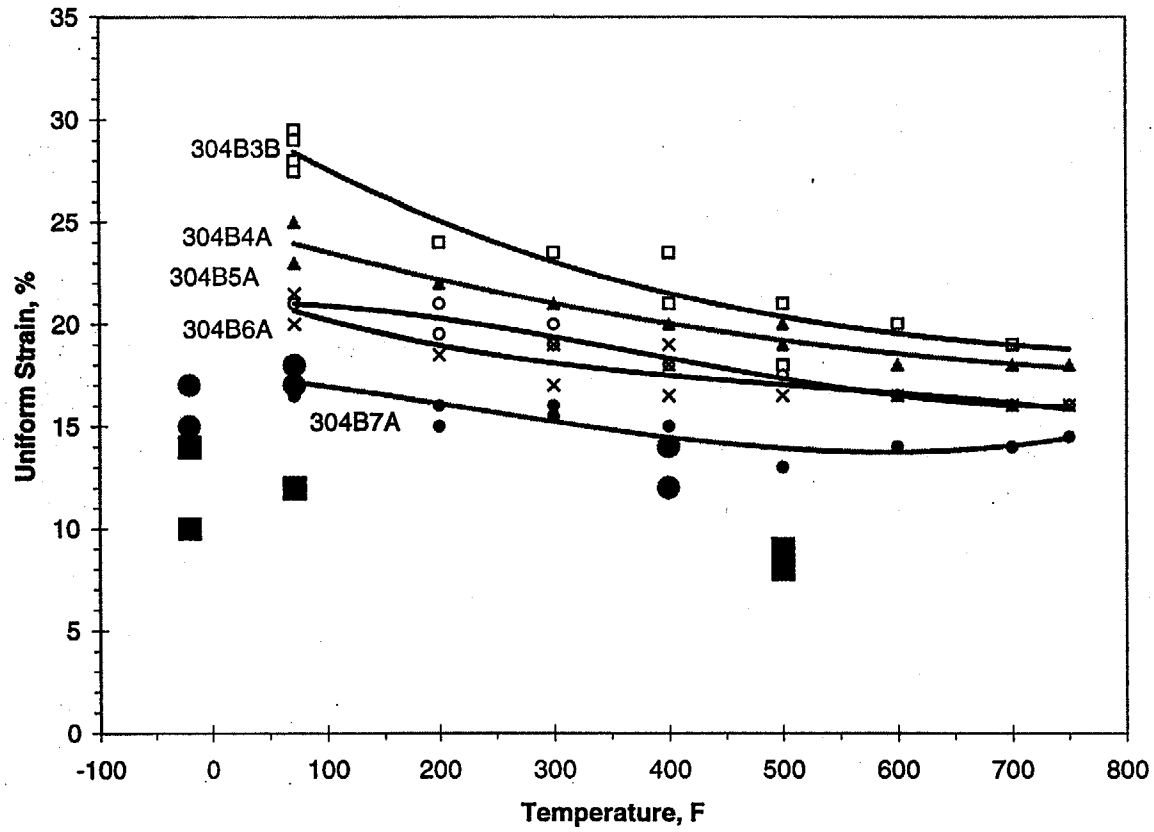


Figure 4-3. Temperature Effects on Elongation of TN-REG and TN-BRP Materials



Room Temperature Fracture Toughness Values

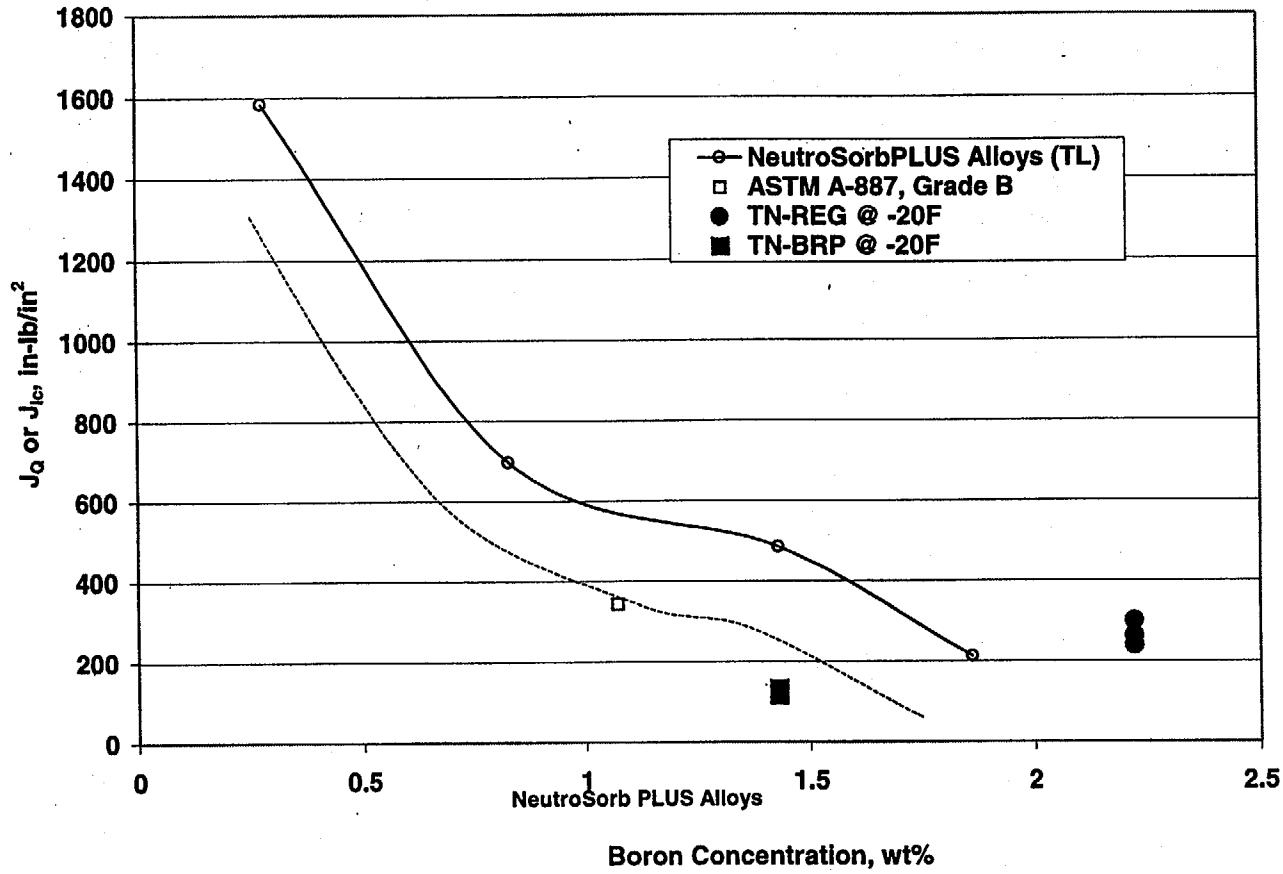


Figure 4-4. Room Temperature Fracture Toughness Values – Borated Stainless Steels
(Data from Westmoreland [3] and from [9])



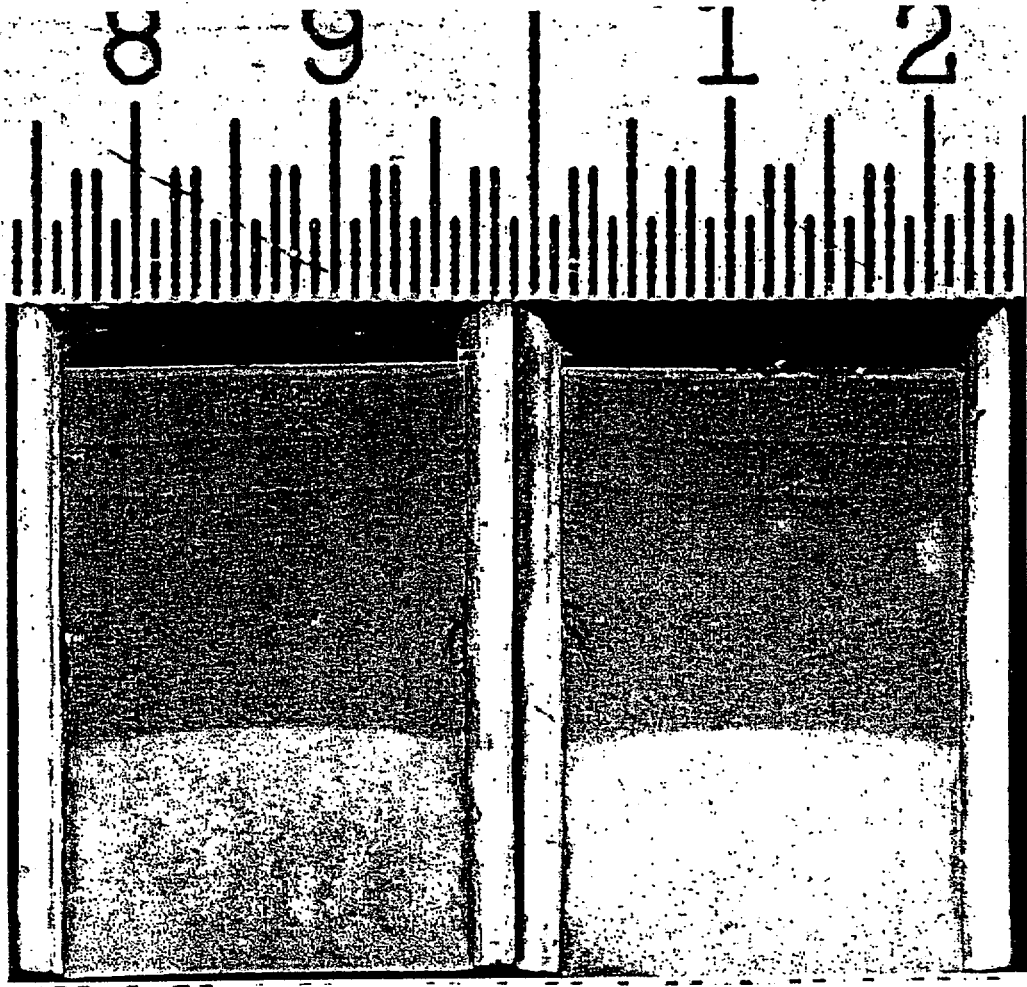


Figure 4-5. Fractography of TN-REG J_k Specimen

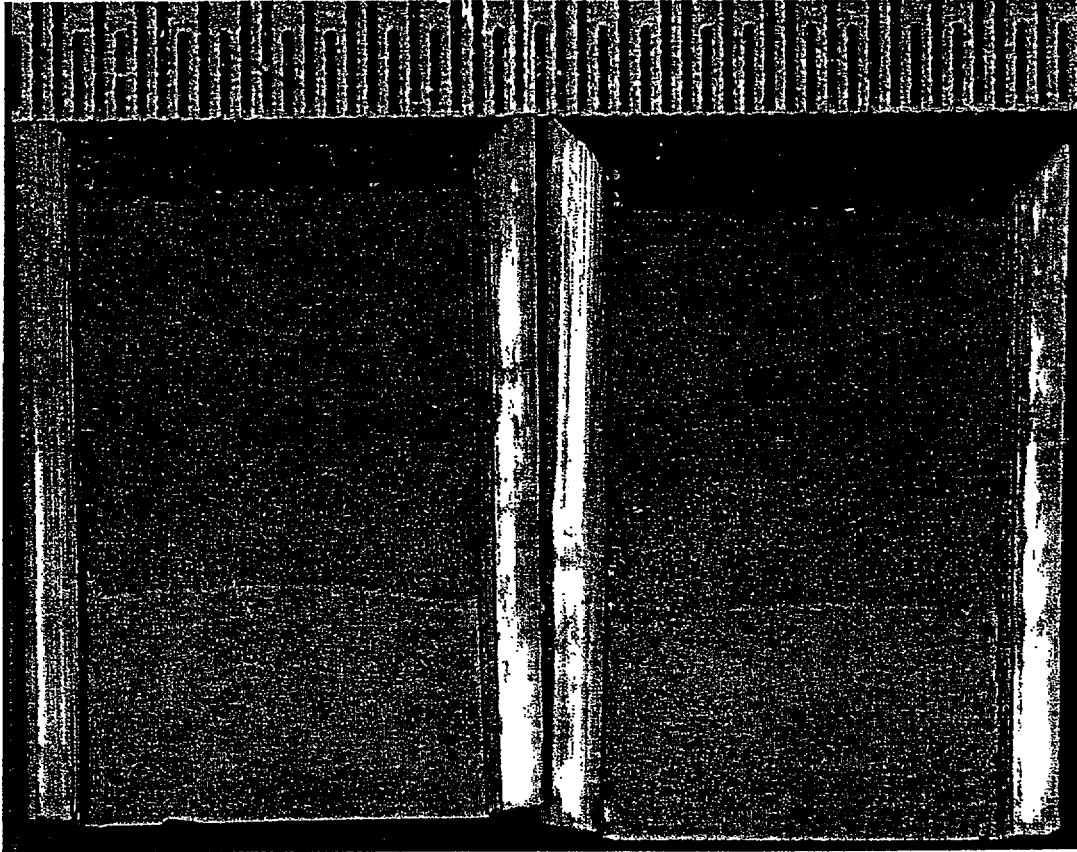


Figure 4-6. Fractography of TN-BRP J_{lc} Specimen

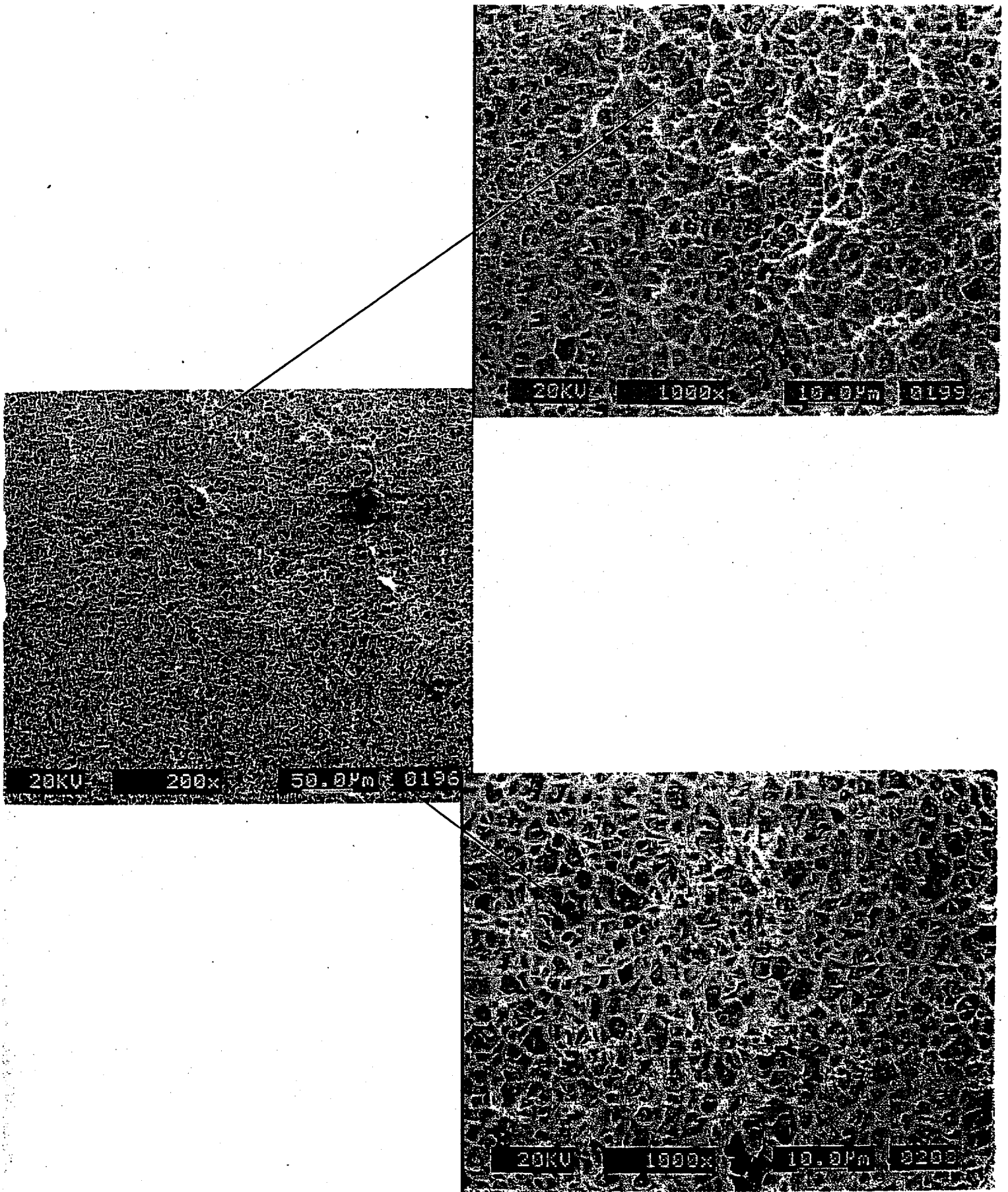


Figure 4-7. Fractography of TN-REG J_c Specimen – High Power

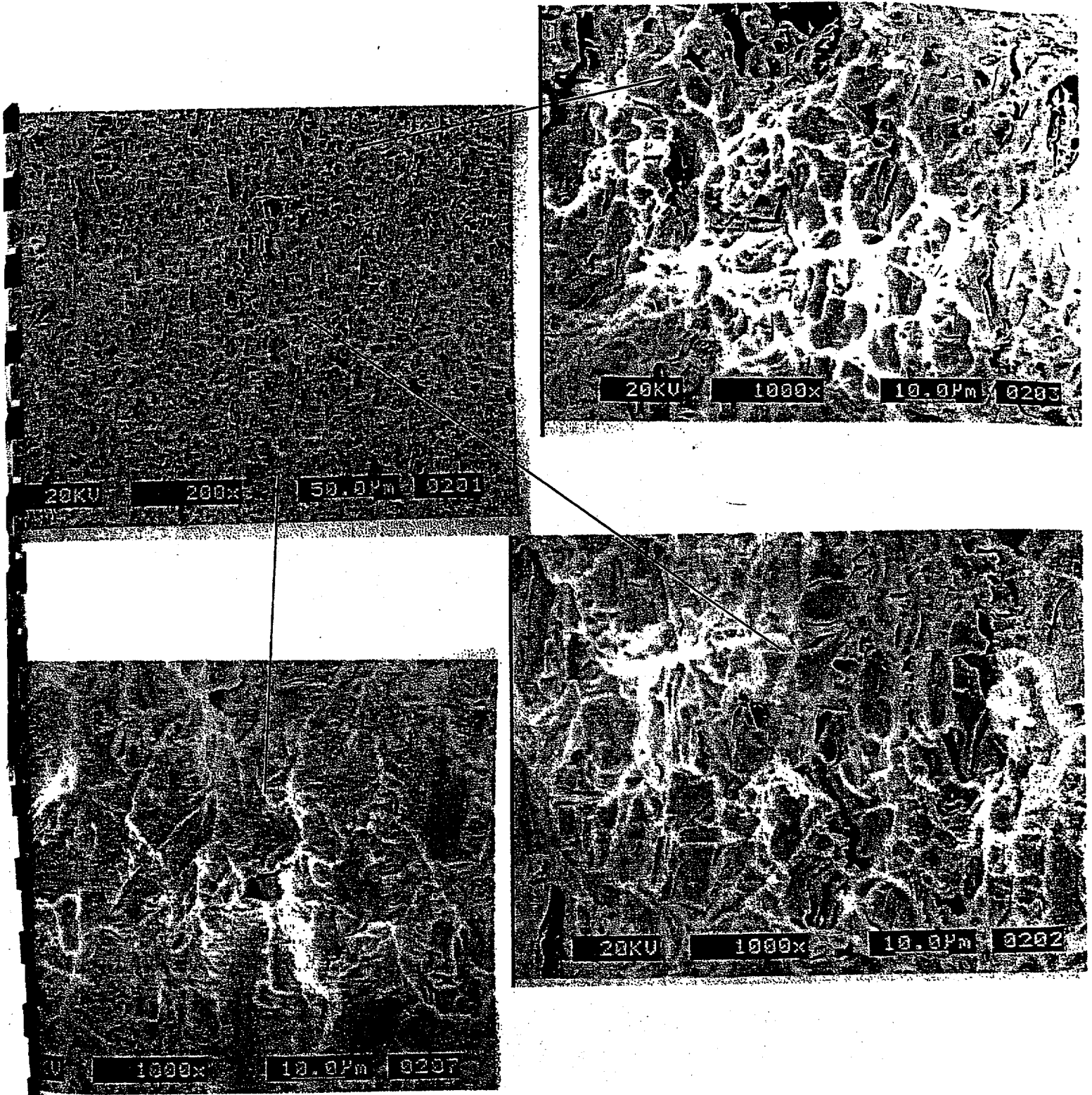
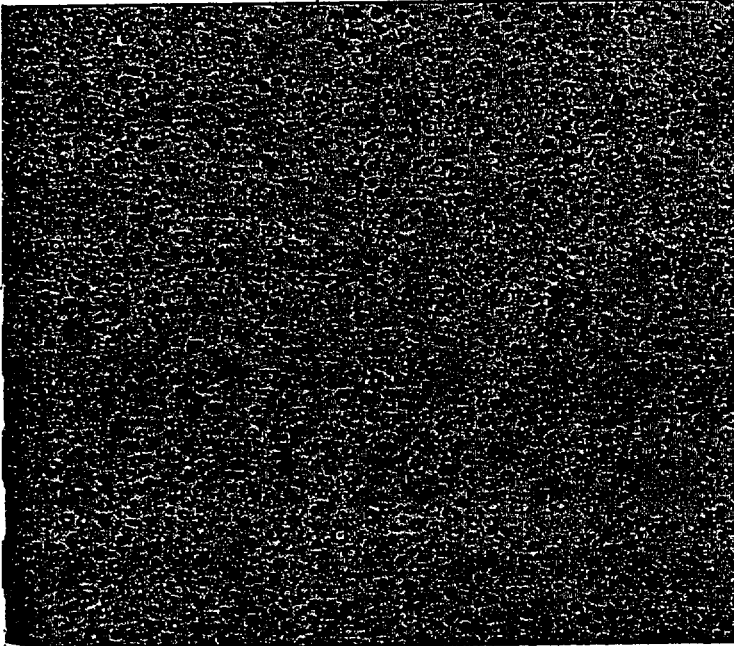


Figure 4-8. Fractography of TN-BRP J_c Specimen – High Power

	Ranges (Objects/Range)	Size (length) (Max.)	Size (width) (Max.)
	Number of particles	Particle size Inches	
Min	Least in one field 937	.000289916	.000244140
Max	Most in one field 1049	.000732421	.000671386
Mean	Average all fields 986.10	.000417608	.000349473
Std.Dev.	36.8848207	.000118701	.000120435
Sum	Total all fields 9861	.004176080	.003494739
# Samples	10	10	10
# Blocks	10	10	10

Field Statistics		Ranges (Objects/Range)	Size (length) (Max.)	Size (width) (Max.)	
Total Scanned Area	.0002458"	Number of particles			
Field Area	.0000245"	Particle size Inches			
Number of Fields	10				
		Field # 1	1049	.000373840	.000259399
		Field # 2	1038	.000343322	.000244140
		Field # 3	974	.000732421	.000671386
		Field # 4	971	.000488281	.000396728
		Field # 5	937	.000289916	.000244140
		Field # 6	948	.000335693	.000259399
		Field # 7	944	.000366210	.000366210
		Field # 8	999	.000366210	.000335693
		Field # 9	1014	.000434875	.000350952
		Field # 10	987	.000445306	.000366687

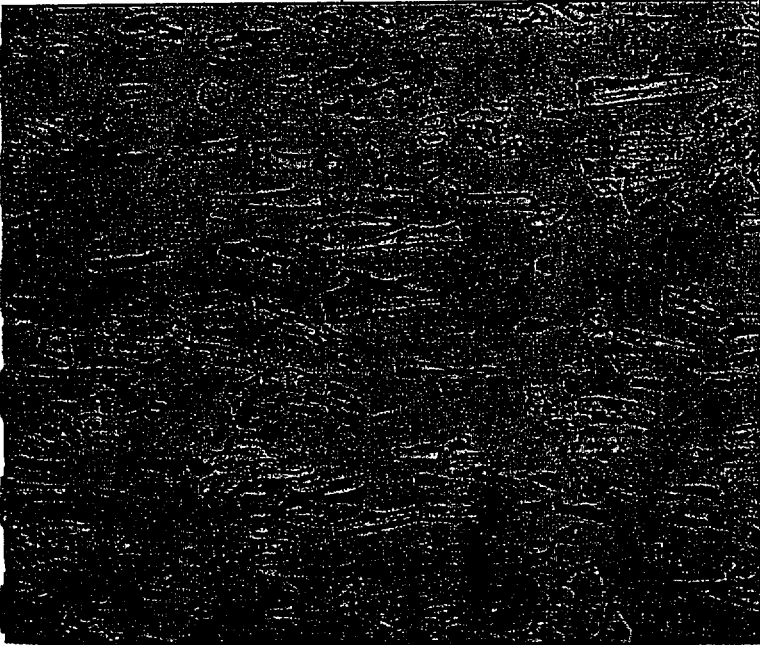
Magnification: 500X

Etchant: 10% KaOH

Figure 4-9. Metallography of TN-REG J_{IC} Specimen

Test Log No. 428829

	Ranges (Objects/Range)	Size (length) (Max.)	Size (width) (Max.)
	Number of particles	Particle size Inches	
Min	Least in one field 303	.000406622	.000213623
Max	Most in one field 725	.001983642	.000854492
Mean	Average all fields 455.90	.001146733	.000522327
Std.Dev.	131.381467	.000440425	.000203067
Sum	Total all fields 4559	.011467337	.005223274
# Samples	10	10	10
# Blocks	10	10	10

Field Statistics		Ranges (Objects/Range)	Size (length) (Max.)	Size (width) (Max.)
		Number of particles	Particle size Inches	
Total Scanned Area	.0002458"			
Field Area	.0000245"			
Number of Fields	10			
	Field # 1	725	.000633239	.000366210
	Field # 2	478	.001305580	.000496864
	Field # 3	363	.001344680	.000854492
	Field # 4	303	.001372337	.000396728
	Field # 5	339	.001983642	.000846862
	Field # 6	358	.001575469	.000671386
	Field # 7	659	.000406622	.000213623
	Field # 8	447	.000885009	.000366210
	Field # 9	481	.000930786	.000423431
	Field # 10	406	.001029968	.000587463

Magnification: 500X

Etchant: 10% KaOH

Figure 4-10. Metallography of TN-BRP J_{IC} Specimen

5.0 DISCUSSION

The materials characterization performed for the TN-REG and TN-BRP plates showed that the tensile properties (including temperature effects), Charpy impact properties, fracture toughness (determined by the J-integral), and microstructure for those borated stainless steel plates were very consistent with the knowledge base that has been generated for borated stainless steels, as summarized in Reference 1.

These tests have demonstrated that the TN-REG and TN-BRP materials are clearly a part of the population of borated stainless steels for which a considerable amount of physical metallurgy and mechanical properties information is available in the published literature.

These tests have also expanded the knowledge base, particularly with respect to fracture toughness.

Although the grades of material that have been accepted for use in Core Support Structures, ASME Nuclear Code Case-N-510-1 [10], do not include the grades that were used in the absorber baskets of the TN-BRP and TN-REG casks, these tests have clearly shown that both the ingot metallurgy material (TN-BRP) and the powder metallurgy product with the highest boron level (TN-REG plates) exhibit properties that are very consistent with the materials that have been accepted for the Code Case.

These test results fit extremely well with projections of properties for the two grades, which heretofore had not been as well characterized.

The ductility and toughness of the borated stainless steels produced by Powder Metallurgy (PM) techniques, as used for the TN-REG basket, were clearly superior to those of the ingot cast and wrought material (e.g., TN-BRP basket material tested).

For the TN-REG and TN-BRP materials, full-size Charpy specimens could not be tested, however, half-size Charpy specimens tested at -20°F gave impact values of 4 ft-lbs and 7 ft-lbs



for the TN-BRP and TN-REG materials, respectively. A first order estimate of the Charpy energy for full size specimens of those materials was done based on their area. That is, estimated Charpy impact energies of 8 ft-lbs and 14 ft-lbs would be expected for the TN-BRP and TN-REG materials. Impact energy for ingot metallurgy borated 304 stainless steel with approximately 1.5% boron, like the TN-BRP material, was estimated to be of the order of 6 ft-lbs or less [1]. Although those Charpy impact energies are not very high, the material still clearly exhibits a reasonable toughness.

Using Charpy impact energy values and correlations between impact energy and K_{Ic} developed for other materials (e.g., pressure vessel steels and other iron-based alloys [11]), where K_{Ic} and K_{ID} are proportional to the square root of the Charpy V-notch impact energy, suggested that the K_{Ic} for material like the TN-REG and TN-BRP basket materials would be of the order of 30 to 70 $ksiv/in$ (Figure 5-1).

Measured J_{Ic} values and K_{Ic} values derived from them showed that the K_{Ic} for TN-BRP material was actually greater than 60 $ksiv/in$ and the K_{Ic} for TN-REG material was about 90 $ksiv/in$.

Metallographic observations also confirmed that the processing of Grade A material seems to do a good job of removing anisotropy. Boride dispersions were generally uniform with fine, spherical particles (Figure 4-9).

The microstructure of the TN-BRP material was consistent with the microstructures reported for other ingot metallurgy products with larger, more elongated, and more angular boride particles (Figure 4-10).

Fractography from J_{Ic} specimens of both grades of material showed a ductile tearing of the austenite matrix between the boride particles and cleavage of the borides themselves. Neither grade exhibited any brittle characteristics.

The characterization program for the TN basket materials is considered to have been a successful demonstration of the predictions of properties based on the literature. Both the TN-REG and

TN-BRP materials were shown to exhibit very predictable tensile strengths and ductilities over the temperature range of interest. The fracture toughness of both alloys was shown to be very reasonable and in good agreement with predictions from the literature and extrapolations based upon other test.

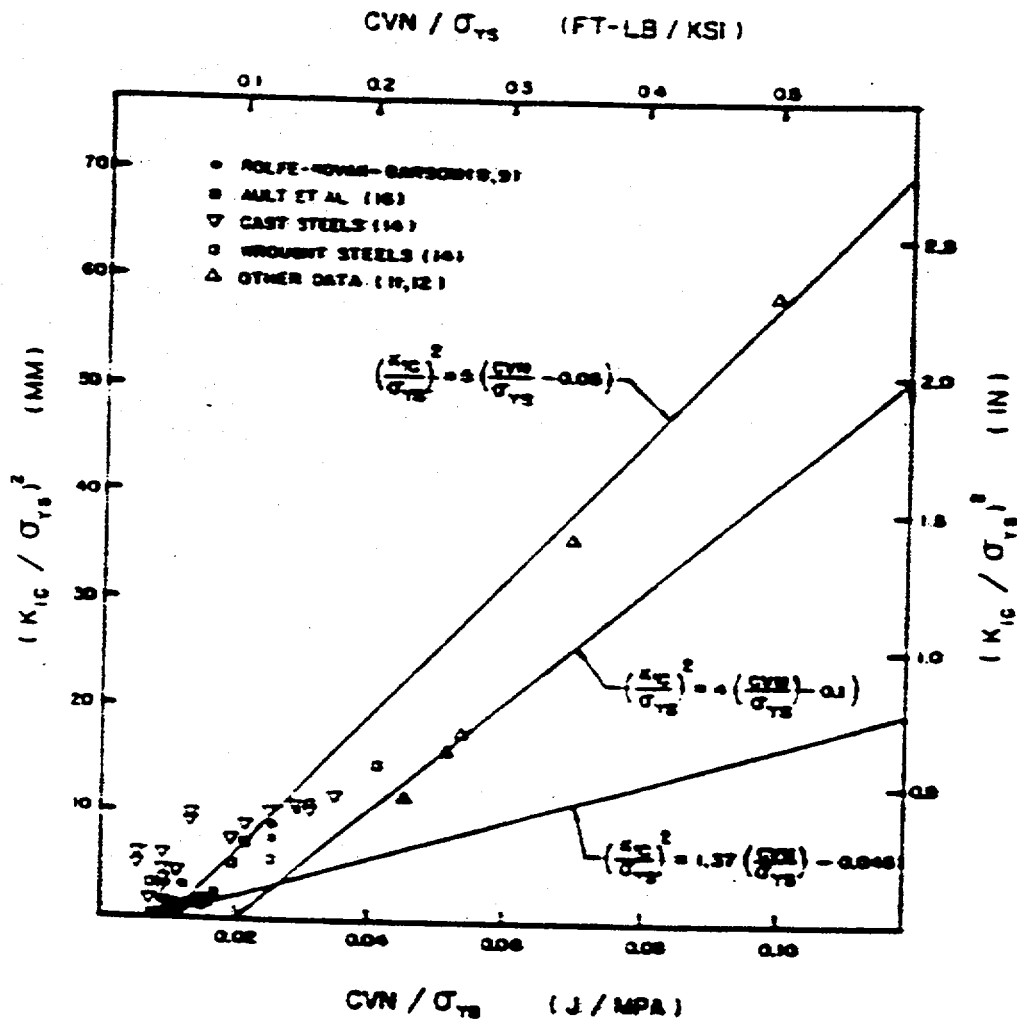


Figure 5-1. Example of Correlations Between K_{Ic} and Charpy Impact Energy (from [11])

6.0 CONCLUSIONS AND RECOMMENDATIONS

The test program required to quantify the basket materials for one-time shipments included tensile tests, Charpy V-notch tests, and J-integral tests using small pre-notched and fatigue pre-cracked bent beams. The Charpy testing demonstrated that the material properties of these plates are consistent with the requirements of the applicable grades of ASTM A-887 borated.

Tests of borated stainless steel plates from the fuel baskets for the Transnuclear TN-REG and TN-BRP shipping and storage casks have demonstrated that plates from both casks have reasonable ductility and fracture toughness.

Plates from the fuel baskets for the TN-REG and TN-BRP casks have shown that the ductility and toughness of borated stainless steels produced by Powder Metallurgy (PM) techniques are clearly superior to those from the ingot cast and wrought material.

Consistent with the literature, temperature appears to exert only a minor effect on tensile strength and ductility. Temperature effects are less for the borated stainless steels than for standard grades such as Type 304L.

Charpy impact test results for half-size Charpy specimens from the TN-REG and TN-BRP materials were consistent with the requirements of ASTM A-887. For the highest boron content materials, the required Charpy impact energy is not very high (about 14 ft-lbs at -20°F).

Charpy impact energy values and correlations between impact energy and K_{Ic} developed for other materials (e.g., pressure vessel steels) suggested that the K_{Ic} for PM 304 with 2% boron (i.e., equivalent to ASTM A-887, Grade 304B7A) would be of the order of 30 to 70 ksi $\sqrt{\text{in}}$. Limited information on J indicates that K_{Ic} 's should range from about 65 to 200 ksi $\sqrt{\text{in}}$.

Measurements of J_{Ic} at -20°F ranged from 116 in-lb/in² to 132 in-lb/in² for the TN-BRP material and 238 in-lb/in² to about 300 in-lb/in² for the TN-REG material. Corresponding K_{Ic} values are 62.4 ksi $\sqrt{\text{in}}$ to 66.4 ksi $\sqrt{\text{in}}$ for the TN-BRP material and 89.4 ksi $\sqrt{\text{in}}$ to 100.4 ksi $\sqrt{\text{in}}$ for the TN-

REG material. The measured J_{Ic} values were in very good agreement with values for similar grades, where the associated K_{Ic} 's range from about 65 to about 125 ksi \sqrt{in} .

Critical linear elastic fracture toughness values (K_{Ic}) calculated from the values of J_{Ic} indicated that lower bound values of K_{Ic} for the actual TN-REG and TN-BRP materials would be 89 ksi \sqrt{in} and about 63 ksi \sqrt{in} , respectively.

All of these measured values of toughness indicate that a reasonable level of toughness would be expected for both the ingot metallurgy material with 1.45% boron (TN-BRP basket) and for the PM material with 2.2% boron (TN-REG)

Optical metallographic examination of the TN-REG and TN-BRP basket materials also demonstrated boride sizes and distributions that were consistent with those reported in the literature, and confirmed that boride morphology, dimensions, and distributions were consistent within a product form.

7.0 REFERENCES

1. G.J. Licina, "Fracture Toughness and Required Testing of Borated Stainless Steels", Structural Integrity Associates report SIR-00-019, February, 2000.
2. "Standard Specification of Borated Stainless Steel Plate, Sheet, and Strip for Nuclear Application", ASTM A-887-88.
3. "Sectioning, Machining, and Testing of Borated Stainless Steel Plates", WMT&R Report 0-02592, Westmoreland Mechanical Testing & Research, Inc., 29 March, 2000.
4. "Standard Test Method for J_{Ic} , A Measure of Fracture Toughness", ASTM E-813-89.
5. "Standard Test Method for J-Integral Characterization of Fracture Toughness", ASTM E-1737-96.
6. Abbott, D. G, Nickell, R. E., "Experience with Certifying Borated Stainless Steel as a Shipping Cask Basket Material", 1st International Topical Meeting on High-level Radioactive Waste Management, 8-12 April, 1990, Las Vegas, NV, CONF-900406.
7. J.J. Stephens, K.B. Sorenson, "Tensile Behavior of Borated Stainless Steels: Phase 1", Government report, SAND-90-1247C, June 1990.
8. C.V. Robino, M.J. Cieslak, "Fusion Welding of Borated Stainless Steels, Final Report: CRADA #CR1042, Sandia national Laboratory, SAND-93-3982, February, 1994.
9. "Borated Stainless Steel Properties", Carpenter Technology. Transmittal from Ian Hunter, Transnucleaire Spent Fuel Interim Storage Department, to Tara Neider, Transnuclear, 12-29-99; received at SI, 1-11-00.
10. "Borated Stainless Steel for Class CS Core Support Structures and Class 1 Component Supports, Section III, Division", ASME Code Case N-510-1 (1994).

11. R. Roberts, C. Newton, "Interpretive Report on Small Scale Test Correlations with K_{Ic} Data",
Welding Research Council Bulletin 265, February, 1981

